JOURNAL OF OPTOELECTRONICS AND ADVANCED MATERIALS Vol. 9, No. 10, October 2007, p. 2973 - 2978

Ovshinsky Lecture

Photon effects in chalcogenide glasses

K. SHIMAKAWA
Department of Electrical and Electronic Engineering, Gifu University, Gifu 501-1193, Japan

Chalcogenide glasses reveal characteristic optoelectronic properties. The photon effects, i.e. photoinduced effects in the other term, are of particular interest from the viewpoint of fundamental science and modern applications. Current understandings of photon effects, e.g. the photodarkening (PD), the photoinduced volume expansion (PVE), and the photoinduced defect creation (PDC), are briefly reviewed. In particular, through the in-situ and simultaneous measurements of these effects, we will discuss direct relation among these PD, PVE, and PDC.

(Received July 3, 2007; accepted October 1, 2007)

Keywords: Chalcogenide glasses, Photoinduced metastability, Photoinduced structural change, Photoinduced optical property, Molecular dynamic simulation, Modern applications

1. Introduction

Ovshinsky's discovery of electrical switching and memory effects in chalcogenide glasses [1] was a milestone event, and the news propagated almost like a "shock wave" among the scientific community. The idea developed at that time (some 40 years ago) has now been realized as DVDs in a huge memory market [2]. Large area TV displays and large area solar cells using hydrogenated amorphous silicon (a-Si:H) are also co-products from this shock-wave. There were various, of course, a number of pioneering works in earlier stages of this field (see for example ref. [3-5]).

Excitingly, an avalanche effect in a-Se films has been discovered and has been applied to the development of an ultrasensitive video (or an image) tube called the Harpicon or the HARP video tube [6]. (The HARP is an acronym for "high-gain avalanche rushing amorphous photoconductor"). Another exciting application of a-Se, and commercially the most significant, is the development of digital x-ray image sensors for medical imaging [7]. It is remarkable that, starting from "Xerography" in 1950s to 1970s, this elemental chalcogenide glass has continued to play a key role in various commercial products: the photocopier, laser printer, HARP video tube, and the x-ray image detector. (Before the advent of xerography, crystalline Se was used in rectifiers, photocells and solar cells, all of which are now obsolete).

Scientific progress in chalcogenide glasses, in my view, has followed two basic ideas on defect structures and topological network structures, which have been recognized to be fundamentally very important: One is a model of *charged dangling bonds* [3,8], and the other is the network constraint theory developed by Phillips [9]. Experimental works related to the above ideas are still continuing to clarify the fundamental physical and chemical properties in chalcogenide glasses.

It is well known that chalcogenide glasses show a metastable photoinduced transformation of structural network and microscopic defect structures [10,27]. These *photon effects*, in particular the photodarkening (PD), the photoinduced volume expansion (PVE), and the photoinduced defect creation (PDC), are still a matter of debate. In the present paper, we will briefly review the current understandings of the photon effects in chalcogenide glasses, through the in-situ and simultaneous measurements of these PD, PVE, and PDC. The results obtained from Molecular Dynamic Simulations are also discussed to elucidate the microscopic view during and after photoillumination.

2. Relations among photodarkening (PD), photoinduced volume expansion (PVE), and photoinduced defect creation (PDC)

Firstly, the time evolution of the changes in the optical absorption coefficient (PD), $\Delta\alpha$, at 1.95 eV during various cycles of Ar laser illumination at 50 and 300 K. in a-As_2Se_3 films is shown in Fig. 1. $\Delta\alpha(t)$ is defined as $\ln (T(0)/T(t))/d$, where d is the film thickness, $T(0)$ the initial optical transmittance and $T(t)$ the transmittance at the time t. The details of the measurements are presented elsewhere [28].

As shown in Fig. 1 (a), $\Delta\alpha$ increases rapidly at first at both temperatures before reaching close to saturation after some time. When the Ar-laser illumination is switched off, a decrease in $\Delta\alpha$ is observed which reaches a constant value quickly. This portion of the total change is the *transient* part induced by illumination and the portion remaining after stopping the illumination is the usually observed metastable PD. The cycling was repeated many times after the metastable state was reached, and every illumination confirmed the occurrence

of only the transient PD. The total increase in Δα, during illumination, is the sum of the transient and the metastable PD. The transient parts of the changes are found to be nearly 60% and 30 % of the total changes induced during illumination at 300 and 50 K, respectively. Fig. 1 (b) shows the initial kinetics of Δα. Δα increases and decreases very rapidly when the illumination is switched on and off, but in neither case does it return the original value, i.e. the metastable photodarkening is accumulated with each successive illumination.

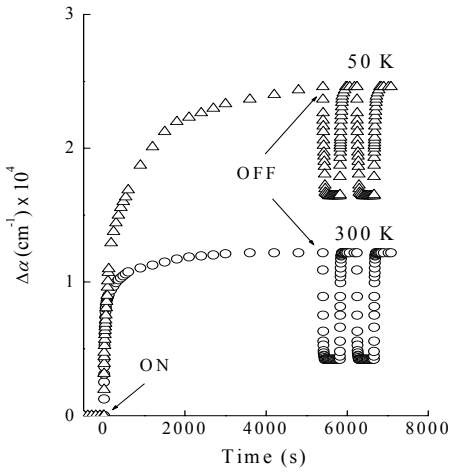

a

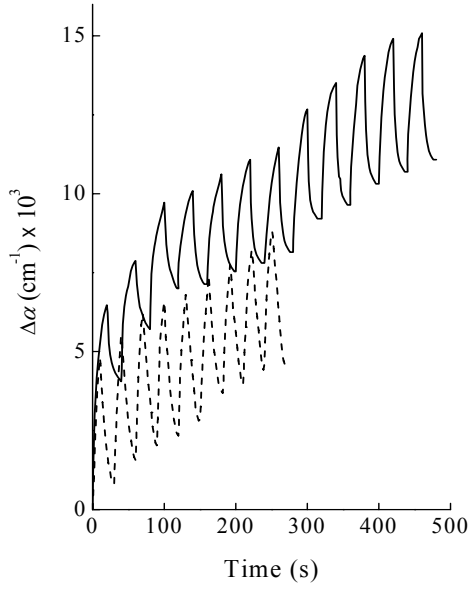

b

Fig. 1. (a) Time evolution of changes in absorption coefficient, Δα, for a-As_2Se_3 films at 50 (△) and 300 K (○). ON and OFF stages of the Ar laser are indicated by the arrows. (b) Δα with time for short-duration illumination for a-As_2Se_3 films at 50 (solid line) and 300 K (dashed line).

Secondary, we will show the typical results of photoinduced volume expansion (PVE). Fig. 2 (a) shows an example of surface height map for *a*-As_2Se_3 films (Si substrate) that is obtained by the measuring system described elsewhere [29]. The time evolution of the changes is shown in Fig. 2 (b). The surface height increased by 10 nm (Δd/d ≈ 2%) in 200 seconds of illumination of laser (532 nm in wave length and 91 mW / cm^2 of power density). After 600 seconds, we turned off the illumination. The surface height started decreasing and settled in 200 seconds at 2 nm less than the height before light off. The PVE is observed during and after illumination. Transient PVE must be involved during illumination, since after illumination is cut off, a slight decrease of the surface height is observed. Remaining increase of surface height after cut off the illumination can be called the metastable PVE. Similar to the PD, the transient PVE is also involved.

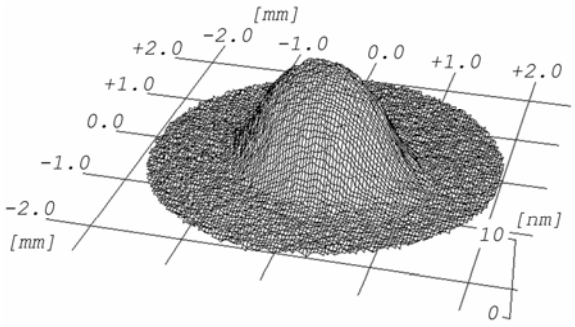

a

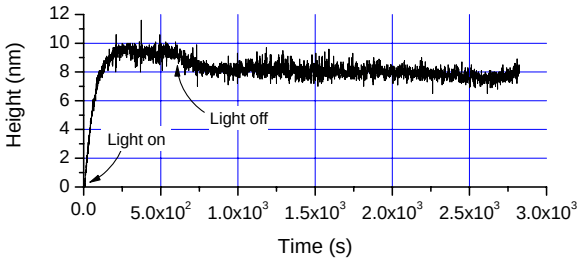

b

Fig. 2. (a) An example of surface height map for flatly deposited As_2Se_3 film (λ = 532 nm, 86 mW/cm^2). Note that the height scale is enlarged about 10^5 times of the horizontal scale. (b) Time evolution of the surface height for flatly deposited a-As_2Se_3.

Thirdly, the photoinduced defect creation (PDC) is discussed using photocurrent degradation in normally and obliquely deposited a-As_2Se_3 films, respectively. Fig. 3 shows the variation of defect creation (N_t/N_0), for (a) bandgap and (b) sub-gap illuminations, respectively, with exposure time estimated from the changes in photocurrent, where N_t/N_0 is the ratio of newly created

number of defect to initially number of defect. Details have been reported elsewhere [30]. All symbols are given in the figure caption. The solid lines are calculated results and are given by a stretched exponential function. N_t increases with time during illumination in obliquely and normally deposited films. It is clear that N_t for obliquely deposited films is always larger than that for normally deposited ones at the same temperature. From this observation it is suggested that the defect creation is more enhanced in obliquely deposited samples than in normally deposited ones.

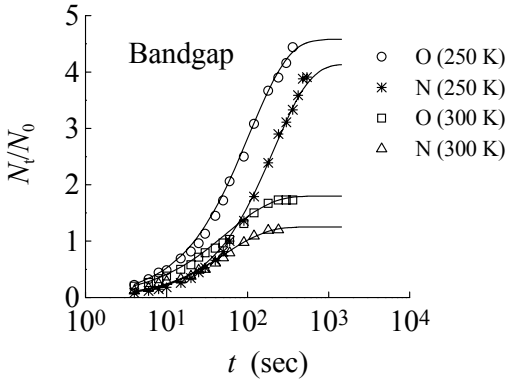

Fig. 3. Variation of N_t/N_0 with exposure time, which is estimated from the changes in photocurrent for bandgap. N and O represent normally and obliquely deposited a-As_2Se_3 films, respectively. Solid curves are calculated results (see the text).

Now, we should discuss relations among phenomena of PD, PVE, and PDC. The relations among these (triangle) are shown in Fig. 4. Are there any direct correlations, one-to-one relation, between PD and PVE, between PD and PDC, and between PDC and PVE ? These are important questions to understand overall features of photon effects.

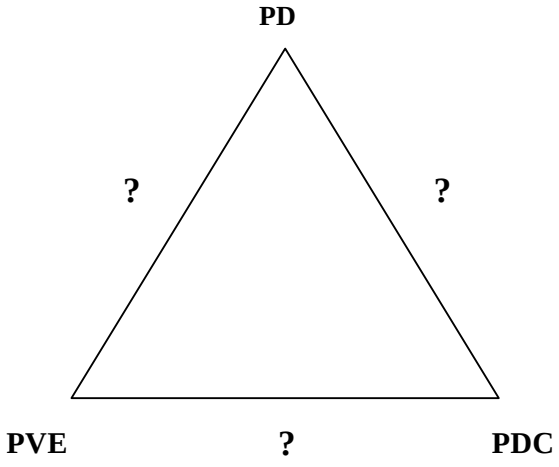

Fig. 4. Direct relationship among PD, PVE, and PDC.

In-situ simultaneous measurements of PD and PVE have been performed [31]. As shown in Fig. 5, the phase-shifting interferometer is employed to measure the PVE. A blue-violet laser (wavelength, $\lambda \sim 405$ nm) is used to improve the accuracy and to avoid multiple reflections in the films. The reference mirror is driven by a PZT actuator with a step of $\lambda/8$ (i.e. $\lambda/4$ of optical path length) directed along the light beam axis to shift the phase of the interference fringes. The interference fringes reflect the surface height variation of the sample. A set of seven images of phase-shifted interference fringes are obtained by the frame grabber to calculate the surface height. To measure the PD, a computer controlled spectroscope is employed. A small probe light beam (~ 0.5 mm in diameter) that is produced by a halogen lamp passes through a pinhole and a collimator lens 2, and is incident on the center of the photodarkened area. Some of the probe light is absorbed by the films, some is reflected on the surface and some is transmitted. The transmitted probe light is decomposed into a spectrum by the grating. The spectrum is directly projected onto the surface of a CCD chip in CCD camera 2.

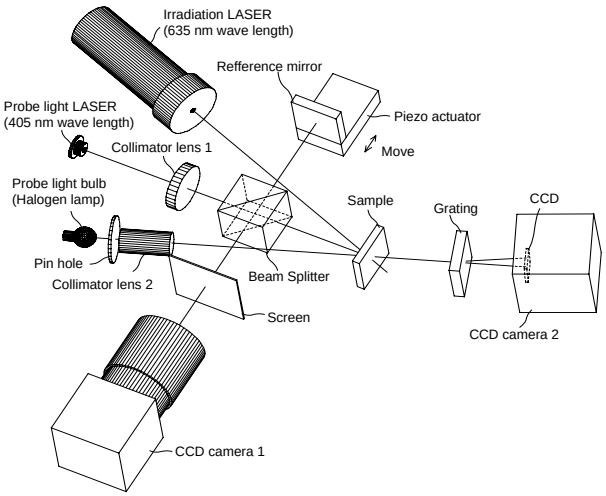

Fig. 5. Setting of in-situ simultaneous measurement system of PD and PVE, with Twyman -Green interferometer and the laser for illumination.

The time evolutions of both the PVE and PD in *a*-As_2Se_3 film, and the surface height maps that is obtained by the surface height measuring system described in the previous section are shown in Fig. 6. The surface height increased by 8.5 nm ($\Delta d/d \approx 1.7$ %) after 1200 seconds of illumination and reached an equilibrium state, while the change in the optical absorption is still taking place. When the illumination was turned off (after illumination of 1500 s), the surface height and $\Delta\alpha$ decreased around 1 nm and 500 cm^{-1}, respectively, from those values just before stopping the illumination. PD and photoinduced volume expansion (PVE: increase of surface height) are observed during and after illumination. Transient PD and transient PVE must be involved during

illumination, since after stopping illumination, slight decreases of $\Delta\alpha$ and Δh are observed. The remaining increases of $\Delta\alpha$ and Δh after the cut off of illumination are the so-called metastable PD and metastable PVE, respectively.

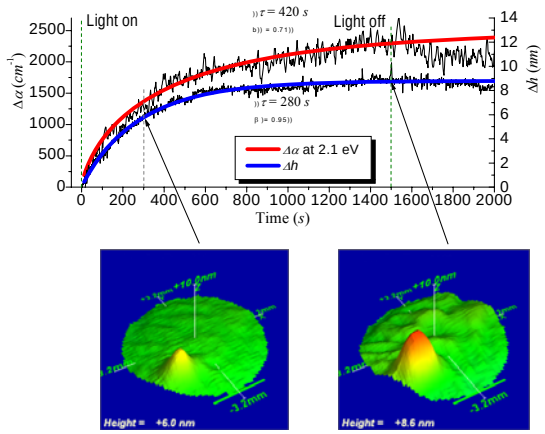

Fig. 6. Time evolution of the $\Delta\alpha$ and Δh for a-As_2Se_3 film (λ = 635 nm, 100 mW/cm^2), and height maps at 300 s and 1500 s after illumination starts.

The PD and PVE are analyzed during the illumination by nonlinear fitting. Both the PD and PVE are presented by the following function:

$$y = A\left[1 - \exp\left\{-\left(\frac{t}{\tau}\right)^{\beta}\right\}\right] \qquad (1)$$

where y is the measured value ($\Delta\alpha$ or Δh) at time t, and A is a constant (equal to the total amount of change), τ and β are, the effective reaction time and the dispersion parameter, respectively. The time evolution of Δh is very close to an exponential function (β is close to 1), while the change in $\Delta\alpha$ at 2.1 eV is given by a typical stretched exponential function (β = 0.71). The effective reaction time τ for Δh and $\Delta\alpha$ are 280 s and 420 s, respectively: This behavior indicates that $\Delta\alpha$ continues to change (increase) even after the changes in Δh saturate. The above results suggest that there is no one-to-one correspondence between PD and PVE.

Next, we will try to measure PDC and PD simultaneously. Using coplanar cells, and using He-Ne laser as an excitation light source, the photocurrent and optical transmittance through the gap between electrodes.

Fig. 7 shows a typical example of the simultaneous measurements of the time evolution of photocurrent I_p and $\Delta\alpha$ in a-As_2Se_3 films [32]. Note that I_p can be inversely proportional to defect density [10,30]. Both the I_p and $\Delta\alpha$ are fitted to the stretched exponential function (see Eq.(1)), while I_p decreases and $\Delta\alpha$ increases with time. The relaxation time τ and the dispersion parameter β deduced from the fitting procedures are 60 s and 0.85, respectively, for the $\Delta\alpha$. On the other hand, τ and β for I_p, respectively, are 0.35 s and 0.25 (more dispersive than the change in $\Delta\alpha$). This clearly shows that PDC occurs more faster than PD. Again, no direct one-to-one correspondence between PD and PDC is suggested here, although there are some proposals of direct correlation between PD and PDC [33,34]. Note that PVC can be monitored by midgap optical absorption as well and hence it is of interest to measure midgap absorption, instead of I_p. Data will be published in a future paper.

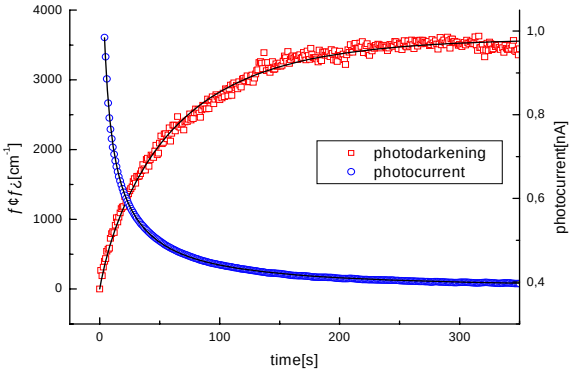

Fig. 7. The simultaneous measurements of the time evolution of photocurrent I_p and $\Delta\alpha$ in a-As_2Se_3 films.

Now, only one question, whether or not PVE correlates with PDC, is remained. Simultaneous measurements of PVE and PDC cannot be easy, if the PDC is monitored by photocurrent. However, as suggested above, PVE and midgap absorption may be not difficult to measure simultaneously. Unfortunately, we have not yet tried it so far.

Finally, we show the theoretical predictions from the tight-binding molecular dynamic dynamics (TBMD) [35]. We made the test run for the eighteen-memberd selenium chain (with 1-dimensional periodic boundary condition). The initial configuration for bond length, bond angle, and dihedral angle, respectively, were 2.36 Å, 100 °, and 98 °. When a photon was absorbed an electron from the highest occupied molecular orbital (HOMO) to the lowest unoccupied molecular orbital (LUMO), one bond length in the chain started to increase and bond-breaking occurred. Two snapshots of this process can be seen in Fig. 8.

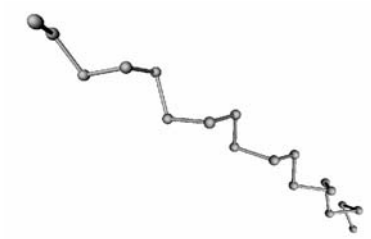

a

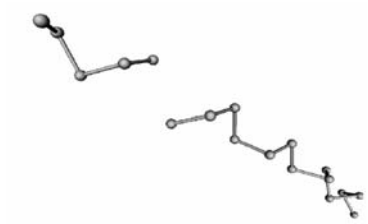

b

Fig. 8. Test run of TBMD simulation for the eighteen-memberd selenium chain (with 1-dimensional periodic boundary condition); (a) before photoillumination, (b) during photoillumination.

The principal results of TBMD simulation for 162 Se-atoms are shown in Figs. 9 and 10 [31]. The time development of photo-induced bond breaking due to an added electron and the corresponding volume expansion in one of amorphous Selenium sample is shown in Fig. 9. Before the excitation at 5 ps the bond length was about 2.55 Å. In this particular case bond breaking occurred at a weaker bond, which had a larger interatomic separation than the majority of the nearest-neighbor bonds of 2.4 Å. During the illumination, this weaker bond (2.55 Å) increased by 10-20 % (in this example to 3 Å) and it decreases to its original value after the de-excitation. (Arrows show the excitation and de-excitations in Fig. 10.) The volume change, calculated from the center-of-mass, follows the bond breaking and it shows damped oscillations on the picoseconds time scale.

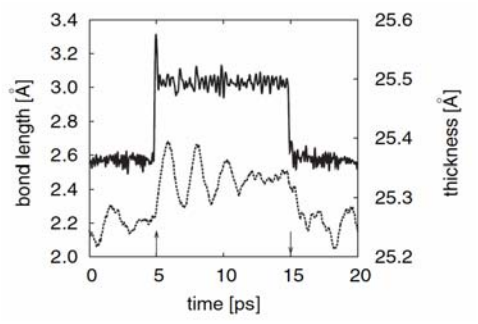

Fig. 9. TBMD simulation for 162 Se-atoms. The time development of photo-induced bond breaking due to an added electron and the corresponding volume expansion in a-Se.

It was found that inter-chain bonds were formed after creating a hole into the HOMO state and they cause contraction of the sample (Fig. 10). This contraction always appears near to atoms where HOMO is localized. Since HOMO is usually localized in the vicinity of a one-fold coordinated atom, the inter-chain bond formation often takes place between a one-fold coordinated atom and a two fold-coordinated atom.

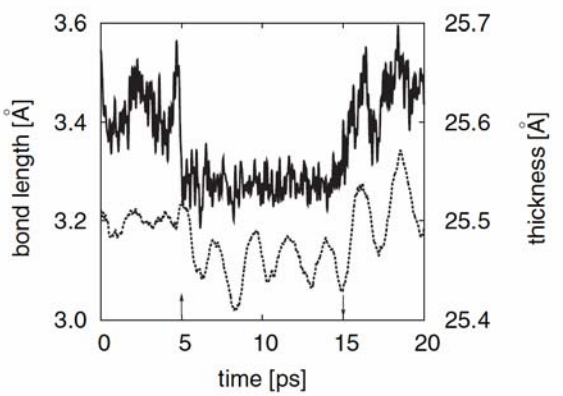

Fig. 10. TBMD simulation for 162 Se-atoms. The time development of photo-induced bond breaking (and bond alternation) due to an added hole into the HOMO state, and the corresponding volume contraction in a-Se.

The above simulation work suggests that the volume expansion is larger than volume contraction and hence we totally observe PVE experimentally. The TBMD simulation shows that both the bond breaking (or bond alternation) (PDC) and the PVE occur simultaneously, suggesting direct correlation between them. Thus the experimental work proposed above may be of interest to reach a conclusion.

3. Summary

Current understandings of photon effects, e.g. the photodarkening (PD), the photoinduced volume expansion (PVE), and the photoinduced defect creation (PDC), in amorphous chalcogenides were briefly reviewed. Recent studies of the in-situ and simultaneous measurements of these effects, suggest that there are no direct relationships among PD, PVE, and PDC, while direct correlation between PVE and PDC has not yet been examined experimentally.

Acknowledgements

I would like to thank Professors R. Grigorovici and M. Popescu for providing me the Ovshinsky Lecture in 3rd Conference of Amorphous and Nanostructured chalcogenides. I also thank many my colleagues, Professors K. Morigaki, T. Aoki, Ke. Tanaka, Jai Singh, S. Kugler, and S. Kasap, E. A. Davis, S.R. Elliott and Drs. A.

V. Kolobov and Y. Ikeda for their very helpful discussions. The part of the present work was supported by the Japan Society of Promotion of Science (JSPS) and the Ministry of Economy, Trade and Industry in Japan.

References

[1] S. R. Ovshinsky, Phys. Rev. Lett. **21**, 1450 (1968).
[2] T. Ohta, S. R. Ovshinsky, Photo-induced Metastability in Amorphous Semiconductors, edited by A. V. Kolobov (Wiley-VCH, Weinheim, 2003) p.310.
[3] N. F. Mott, E. A. Davis, Electronic Processes in Non-Crystalline Materials 2nd ed. (Oxford University Press, Oxford, 1979).
[4] R. Grigorovici, Amorphous and Liquid Semiconductors, edited by J. Tauc (Plenum Press, London and New York, 1974) p.45.
[5] H. Fritzshe, Amorphous and Liquid Semiconductors, edited by J. Tauc (Plenum Press, London and New York, 1974) p.221.
[6] K. Tanioka, J. Yamazaki, K. Shidara, K. Taketoshi, T. Kawamura, S. Ishioka, Y. Takasaki, IEEE Electron Device Letters EDL-**8**, 392 (1987).
[7] S. Kasap, J. A. Rowlands, Proc. IEEE **90**, 591 (2002).
[8] M. A. Kastner, D. Adler, H. Fritzshe, Phys. Rev. Lett. **37**, 1504 (1976).
[9] J. C. Phillips, J. Non-Cryst. Solids **34**, 153 (1979).
[10] K. Shimakawa, A. V. Kolobov, S. R. Elliott, Adv. Phys. **44**, 475 (1995).
[11] J. Dikova, Tz. Babeva, P. Sharlandjiev, J. Optoelectron Adv. Mater. **7**(1), 361 (2005).
[12] M. L. Trunov, S. N. Dub, R. S. Shmegera, J. Optoelectron Adv. Mater. **7**(2), 619 (2005).
[13] N. Starbov, K. Starbova, J. Optoelectron Adv. Mater. **7**(3), 1197 (2005).
[14] M. L. Trunov, J. Optoelectron Adv. Mater. **7**(3), 1223 (2005).
[15] D. Arsova, E. Skordeva, V. Pamukchieva, E. Vateva, J. Optoelectron Adv. Mater. **7**(3), 1259 (2005).
[16] J. Dikova, Tz. Babeva, Tz. Iliev, J. Optoelectron Adv. Mater. **7**(3), 1281 (2005).
[17] J. Tasseva, K. Petkov, D. Kozhuharova, J. Optoelectron Adv. Mater. **7**(3), 1287 (2005).
[18] J. Hegedus, K. Kohary, S. Kugler, J. Optoelectron Adv. Mater. **7**(2), 2231 (2005).
[19] K. Tanaka, J. Optoelectron Adv. Mater. **7**(5), 2571 (2005).
[20] J. Dikova, J. Optoelectron Adv. Mater. **7**(6), 2945 (2005).
[21] M. Kincl, K. Petkov, L. Tichy, J. Optoelectron Adv. Mater. **8**(2), 780 (2006).
[22] Qiming Liu, Xiu Jian Zhoo, Funi Gan, J. Optoelectron Adv. Mater. **8**(5), 1838 (2006).
[23] O. Shpotyuk, V. Balitska, J. Optoelectron Adv. Mater. **8**(6), 2070 (2006).
[24] K. Shimakawa, Y. Ikeda, J. Optoelectron Adv. Mater. **8**(6), 2097 (2006).
[25] Y. Sakaguchi, K. Tamura, J. Optoelectron Adv. Mater. **8**(6), 2101 (2006).
[26] K. Tanaka, A. Saitoh, N. Terakado, J. Optoelectron Adv. Mater. **8**(6), 2058 (2006).
[27] Jai Singh, K. Shimakawa, Advances in Amorphous Semiconductors (CRC Press, London and New York, 2003).
[28] A. Ganjoo, K. Shimakawa, K. Kitano, E. A. Davis, J. Non-Cryst. Solids **299-302**, 917 (2002).
[29] Y. Ikeda, K. Shimakawa, J. Non-Cryst. Solids **338-340**, 539 (2004).
[30] K. Shimakawa, Meherun-Nessa, H. Ishida, A. Ganjoo, Philos. Mag. B **84**, 81 (2004).
[31] Y. Ikeda, K. Shimakawa, Chalcogenide Letters **2**, 125 (2005); J. Non-Cryst. Solids **352**, 1582 (2006).
[32] T. Mori, A. Hosokawa, K. Shimakawa, J. Non-Cryst. Solids (to be published)
[33] A. V. Kolobov, H. Oyanagi, K. Tanaka, Ke. Tanaka, Phys. Rev. B **55**, 726 (1997).
[34] Jai Singh, J. Non-Cryst. Solids (to be published).
[35] J. Hegedus, K. Kohary, D. G. Pettifor, K. Shimakawa, S. Kugler, Phys. Rev. Lett. **95**, 206803 (2005).

*Corresponding author: koichi@cc.gifu-u.ac.jp